

(AGN)²

5. Comparison of Theory with Observations

Week 6

April 8 (Monday), 2024

updated on 04/07, 23:35

선광일 (Kwangil Seon)
KASI / UST

5.1 Introduction

- We are now in a position to compare the theory with the available observations.
- Temperature
 - Intensity ratios of pairs of emission line — emitted by a single ion from two levels with considerably different excitation energies.
 - The relative strengths of H recombination lines vary weakly with T . However, the ratio of the line intensity to the recombination continuum intensity varies more rapidly and can be used to measure T .
 - Combining long- and short-wavelength continuum, which has large and small optical depths, respectively.
 - Long-wavelength continuum and optical-line observations
- Electron density
 - Intensity ratios of other pairs of lines — emitted by a single ion from two levels with nearly the same energy but with different radiative-transition probabilities.
 - Relative strengths of the radio recombination lines (both the density and temperature).
- Information on the involved stars
 - If a nebula is optically thick to a particular type of ionizing radiation, then the total number of photons of this type emitted by the star can be determined from its observational properties.
 - FUV ionizing radiation, optical measurements of the stars, a long base-line color index that gives information on the temperature of the stars.
- Abundance
 - Once the T and ρ are known, the observed strength of a line gives information on the total number of ions, and thus the abundances of the elements.

5.2 Temperature Measurements from Emission Lines

- Ions that have two different upper levels with considerable different excitation energies.
 - [O III] $\lambda 4363$ occurs from the upper 1S , while [O III] $\lambda 4959$ and $\lambda 5007$ occur from the intermediate 1D level. The relative rates of excitation to the 1S and 1D levels depend very strongly on T .

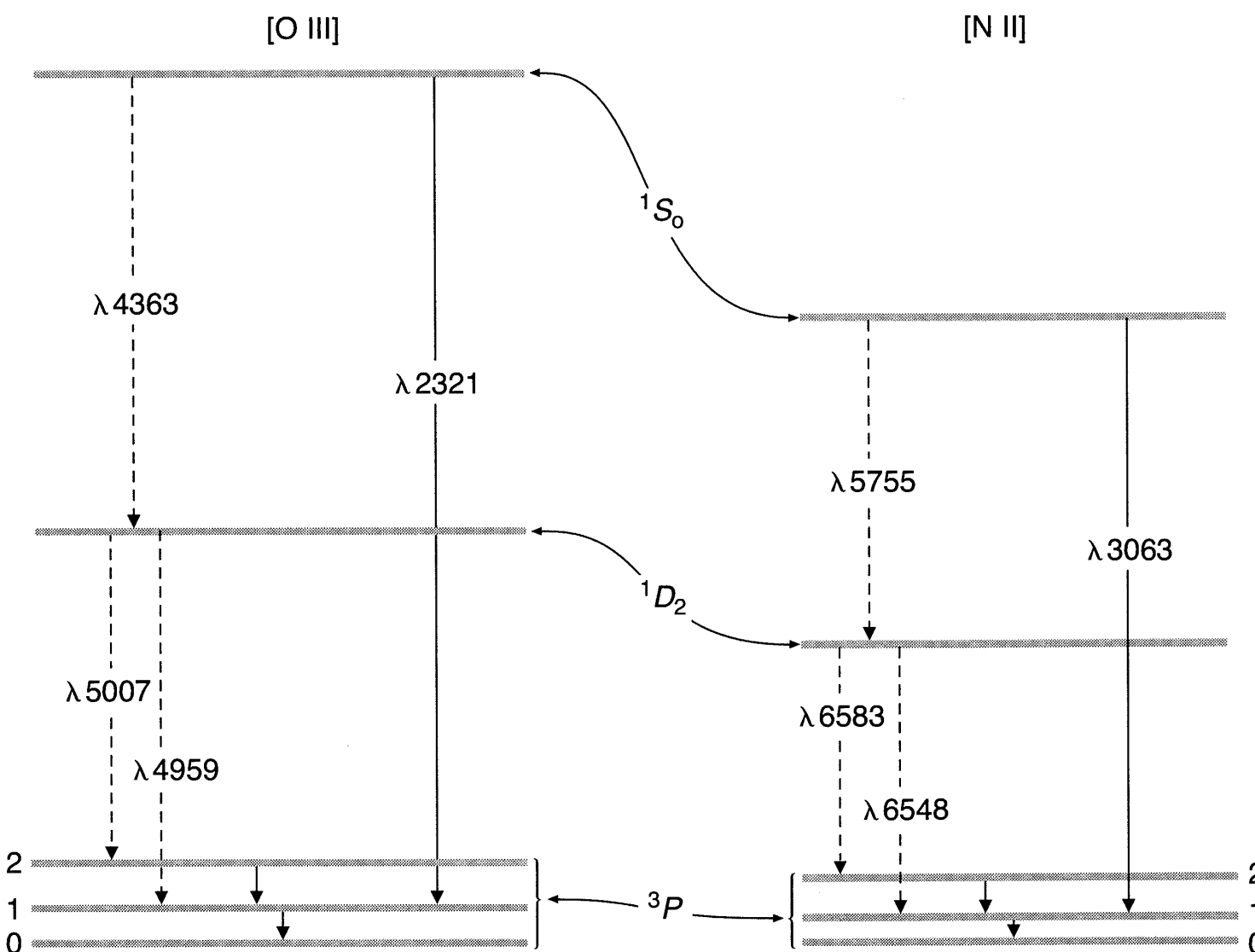
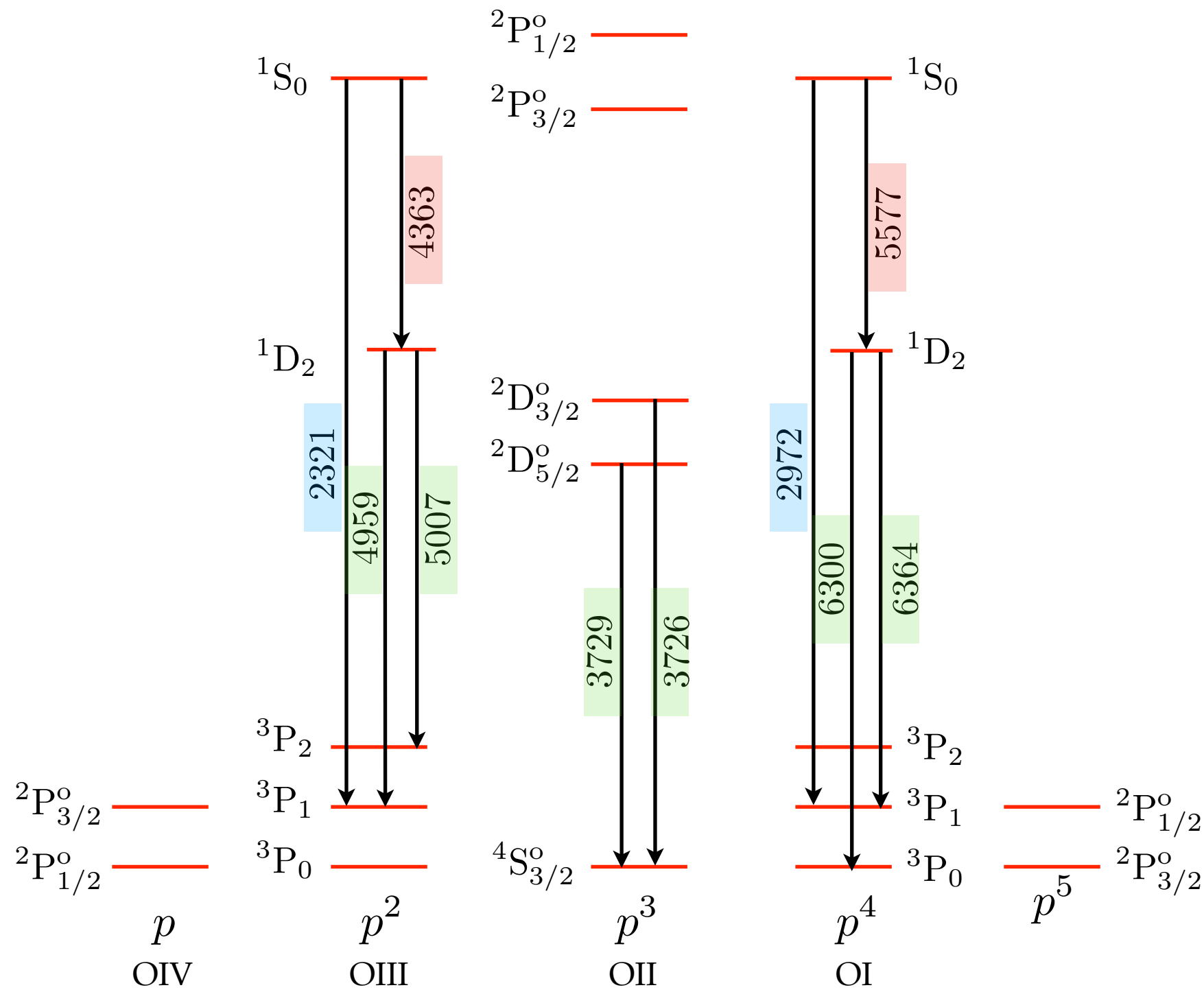


Figure 3.1



- In the low-density limit (no collisional deexcitation):

- $3 \rightarrow 2$ and $3 \rightarrow 1$ transitions:

$$4\pi j(3 \rightarrow 2) = n_e n_P \left(k_{P3} + k_{P4} \frac{A_{43}}{A_{43} + A_{41}} \right) \frac{A_{32}}{A_{32} + A_{31}} h\nu_{32}$$

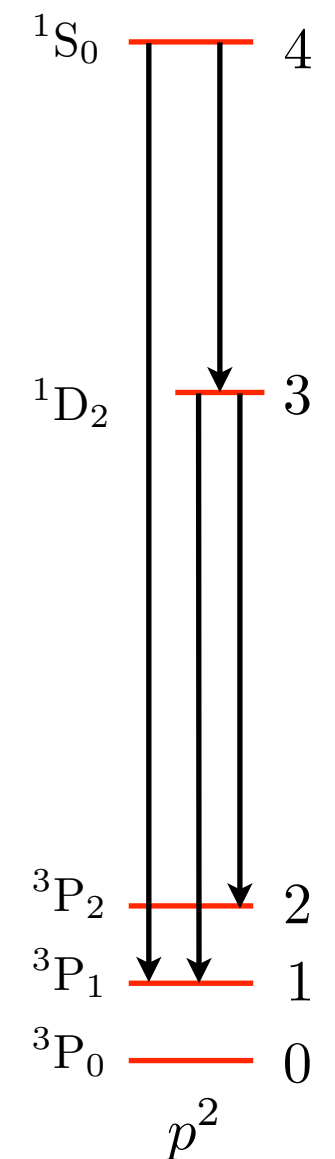
$$4\pi j(3 \rightarrow 1) = n_e n_P \left(k_{P3} + k_{P4} \frac{A_{43}}{A_{43} + A_{41}} \right) \frac{A_{31}}{A_{32} + A_{31}} h\nu_{31}$$

These terms are negligible.

Here, P indicates ${}^3P_{0,1,2}$ levels as a whole

- $4 \rightarrow 3$ transition:

$$4\pi j(4 \rightarrow 3) = n_e n_P k_{P4} \frac{A_{43}}{A_{43} + A_{41}} h\nu_{43}$$



Combining these equations, we obtain

$$\frac{j(3 \rightarrow 1) + j(3 \rightarrow 2)}{j(4 \rightarrow 3)} = \frac{\bar{\nu}}{\nu_{43}} \frac{A_{43} + A_{41}}{A_{43}} \frac{k_{P3}}{k_{P4}} \left(1 + \frac{k_{P4}}{k_{P3}} \frac{A_{43}}{A_{43} + A_{41}} \right) \quad \text{where } \bar{\nu} \equiv \frac{A_{32}\nu_{32} + A_{31}\nu_{31}}{A_{32} + A_{31}}$$

$k_{0u} = \frac{\beta}{T^{1/2}} \frac{\langle \Omega_{u0} \rangle}{g_0} e^{-E_{u0}/kT_{\text{gas}}}$

\downarrow

$$\frac{k_{P3}}{k_{P4}} = \frac{\langle \Omega_{3P} \rangle}{\langle \Omega_{4P} \rangle} \frac{e^{-h\nu_{30}/kT}}{e^{-h\nu_{40}/kT}} = \frac{\langle \Omega_{3P} \rangle}{\langle \Omega_{4P} \rangle} e^{h\nu_{43}/kT} \quad (\text{where } \nu_{43} = \nu_{40} - \nu_{30})$$

$$\begin{aligned} \frac{j(3 \rightarrow 1) + j(3 \rightarrow 2)}{j(4 \rightarrow 3)} &= \frac{\bar{\nu}}{\nu_{43}} \frac{A_{43} + A_{41}}{A_{43}} \frac{\langle \Omega_{30} \rangle}{\langle \Omega_{40} \rangle} e^{h\nu_{43}/kT} \left(1 + \frac{\langle \Omega_{40} \rangle}{\langle \Omega_{30} \rangle} \frac{A_{43}}{A_{43} + A_{41}} e^{-h\nu_{43}/kT} \right) \\ &\simeq \frac{\bar{\nu}}{\nu_{43}} \frac{A_{43} + A_{41}}{A_{43}} \frac{\langle \Omega_{30} \rangle}{\langle \Omega_{40} \rangle} e^{h\nu_{43}/kT} \end{aligned}$$

Note $\langle \Omega_{4P} \rangle < \langle \Omega_{3P} \rangle$ and $e^{-h\nu_{43}/kT} \ll 1$

Thus, the second term inside the parenthesis is negligible.

$$\begin{aligned} \frac{j(3 \rightarrow 1) + j(3 \rightarrow 2)}{j(4 \rightarrow 3)} &= \frac{\bar{\nu}}{\nu_{43}} \frac{A_{43} + A_{41}}{A_{43}} \frac{\langle \Omega_{3P} \rangle}{\langle \Omega_{4P} \rangle} e^{h\nu_{43}/kT} \left(1 + \frac{\langle \Omega_{4P} \rangle}{\langle \Omega_{3P} \rangle} \frac{A_{43}}{A_{43} + A_{41}} e^{-h\nu_{43}/kT} \right) \\ &\simeq \frac{\bar{\nu}}{\nu_{43}} \frac{A_{43} + A_{41}}{A_{43}} \frac{\langle \Omega_{3P} \rangle}{\langle \Omega_{4P} \rangle} e^{h\nu_{43}/kT} \end{aligned}$$

$$\frac{j(3 \rightarrow 1) + j(3 \rightarrow 2)}{j(4 \rightarrow 3)} \simeq \frac{\bar{\nu}}{\nu_{43}} \frac{A_{43} + A_{41}}{A_{43}} \frac{\langle \Omega_{3P} \rangle}{\langle \Omega_{4P} \rangle} e^{h\nu_{43}/kT}$$

Dependence of collision strength on temperature is very weak.
So, we will adopt a typical value.

[O III]	$\langle \Omega_{3P} \rangle = 2.29$	$A_{32} = 2.0 \times 10^{-2} \text{ [s}^{-1}\text{]}$
	$\langle \Omega_{4P} \rangle = 0.29$	$A_{31} = 6.8 \times 10^{-3} \text{ [s}^{-1}\text{]}$
	$\langle \Omega_{43} \rangle = 0.58$	$A_{43} = 1.6 \text{ [s}^{-1}\text{]}$
	$E_{40}/k = 61207 \text{ [K]}$	$A_{41} = 2.3 \times 10^{-1} \text{ [s}^{-1}\text{]}$
	$E_{30}/k = 29169 \text{ [K]}$	$g_3 = 5$
	$E_{20}/k = 441 \text{ [K]}$	$g_4 = 1$
	$E_{10}/k = 163 \text{ [K]}$	
[N II]	$\langle \Omega_{3P} \rangle = 2.64$	$A_{32} = 3.0 \times 10^{-3} \text{ [s}^{-1}\text{]}$
	$\langle \Omega_{4P} \rangle = 0.29$	$A_{31} = 9.8 \times 10^{-4} \text{ [s}^{-1}\text{]}$
	$\langle \Omega_{43} \rangle = 0.83$	$A_{43} = 1.0 \text{ [s}^{-1}\text{]}$
	$E_{40}/k = 47033 \text{ [K]}$	$A_{41} = 3.3 \times 10^{-2} \text{ [s}^{-1}\text{]}$
	$E_{30}/k = 22037 \text{ [K]}$	$g_3 = 5$
	$E_{20}/k = 188 \text{ [K]}$	$g_4 = 1$
	$E_{10}/k = 70 \text{ [K]}$	

Table 3.6 Collision Strength

Ion	$^3P, ^1D$	$^3P, ^1S$	$^1D, ^1S$
N ⁺	2.64	0.29	0.83
O ⁺²	2.29	0.29	0.58

Table 3.12 Transition probabilities

Transition	[N II]		[O III]	
	$A \text{ (s}^{-1}\text{)}$	$\lambda \text{ (\AA)}$	$A \text{ (s}^{-1}\text{)}$	$\lambda \text{ (\AA)}$
$^1D_2 - ^1S_0$	1.0	5754.6	1.6	4363.2
$^3P_2 - ^1S_0$	1.3×10^{-4}	3070.8	6.1×10^{-4}	2331.4
$^3P_1 - ^1S_0$	3.3×10^{-2}	3062.8	2.3×10^{-1}	2321.0
$^3P_2 - ^1D_2$	3.0×10^{-3}	6583.4	2.0×10^{-2}	5006.9
$^3P_1 - ^1D_2$	9.8×10^{-4}	6548.0	6.8×10^{-3}	4958.9
$^3P_0 - ^1D_2$	3.6×10^{-7}	6527.1	1.7×10^{-6}	4931.1

We obtain the line ratio as a function of temperature.

$$\frac{[\text{O III}] 4960 + 5008}{[\text{O III}] 4364} = 8.12 e^{3.20 \times 10^4/T}$$

$$\frac{[\text{N II}] 6549 + 6585}{[\text{N II}] 5756} = 8.23 e^{2.50 \times 10^4/T}$$

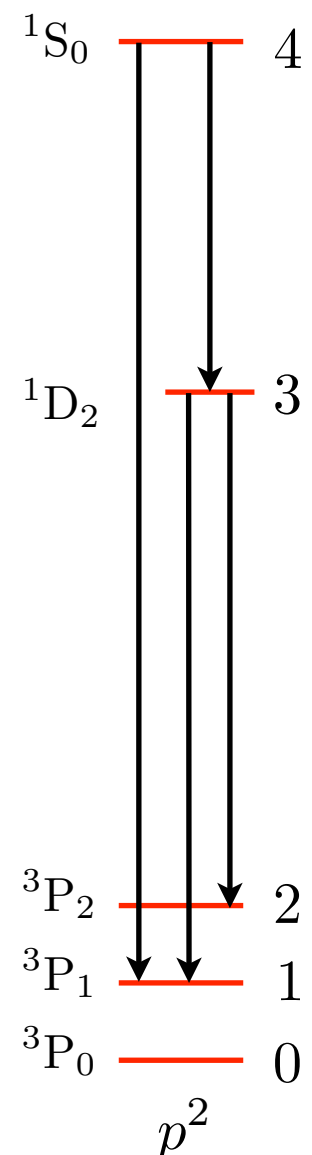
The discrepancy in numerical values within the [O III] formula arise from the differences in the adopted energy level values.

- Collisional effects:
 - The above equations are good approximation up to $n_e \approx 10^5 \text{ cm}^{-3}$. At higher densities, collisional deexcitation begins to play a role.
 - The lower 1D term (level 3) has a considerably longer radiative lifetime than the highest 1S term (level 4), so it is collisionally deexcited at lower electron densities than 1S (level 4), thus weakening $\lambda 4959$ and $\lambda 5007$.
 - In addition, collisional excitation of 1S (level 4) from the excited 1D level (level 3) begins to strengthen $\lambda 4363$.

$$4\pi j(3 \rightarrow 2) = n_e n_P \left(k_{P3} + k_{P4} \frac{A_{43} + n_e k_{43}}{A_{43} + A_{41} + n_e k_{43} + n_e k_{41}} \right) \frac{A_{32}}{A_{32} + A_{31} + n_e k_{32} + n_e k_{31}} h\nu_{32}$$

$$4\pi j(3 \rightarrow 1) = n_e n_P \left(k_{P3} + k_{P4} \frac{A_{43} + n_e k_{43}}{A_{43} + A_{41} + n_e k_{43} + n_e k_{41}} \right) \frac{A_{31}}{A_{32} + A_{31} + n_e k_{32} + n_e k_{31}} h\nu_{31}$$

$$4\pi j(4 \rightarrow 3) = n_e n_P k_{P4} \frac{A_{43}}{A_{43} + A_{41} + n_e k_{43} + n_e k_{41}} h\nu_{43}$$



$$9 \\$$

$$4\pi j(3 \rightarrow 2) = n_e n_P \left(k_{P3} + k_{P4} \frac{A_{43} + n_e k_{43}}{A_{43} + A_{41} + n_e k_{43} + n_e k_{41}} \right) \frac{A_{32}}{A_{32} + A_{31} + n_e k_{32} + n_e k_{31}} h\nu_{32}$$

$$4\pi j(3 \rightarrow 1) = n_e n_P \left(k_{P3} + k_{P4} \frac{A_{43} + n_e k_{43}}{A_{43} + A_{41} + n_e k_{43} + n_e k_{41}} \right) \frac{A_{31}}{A_{32} + A_{31} + n_e k_{32} + n_e k_{31}} h\nu_{31}$$

$$4\pi j(4 \rightarrow 3) = n_e n_P k_{P4} \frac{A_{43}}{A_{43} + A_{41} + n_e k_{43} + n_e k_{41}} h\nu_{43}$$

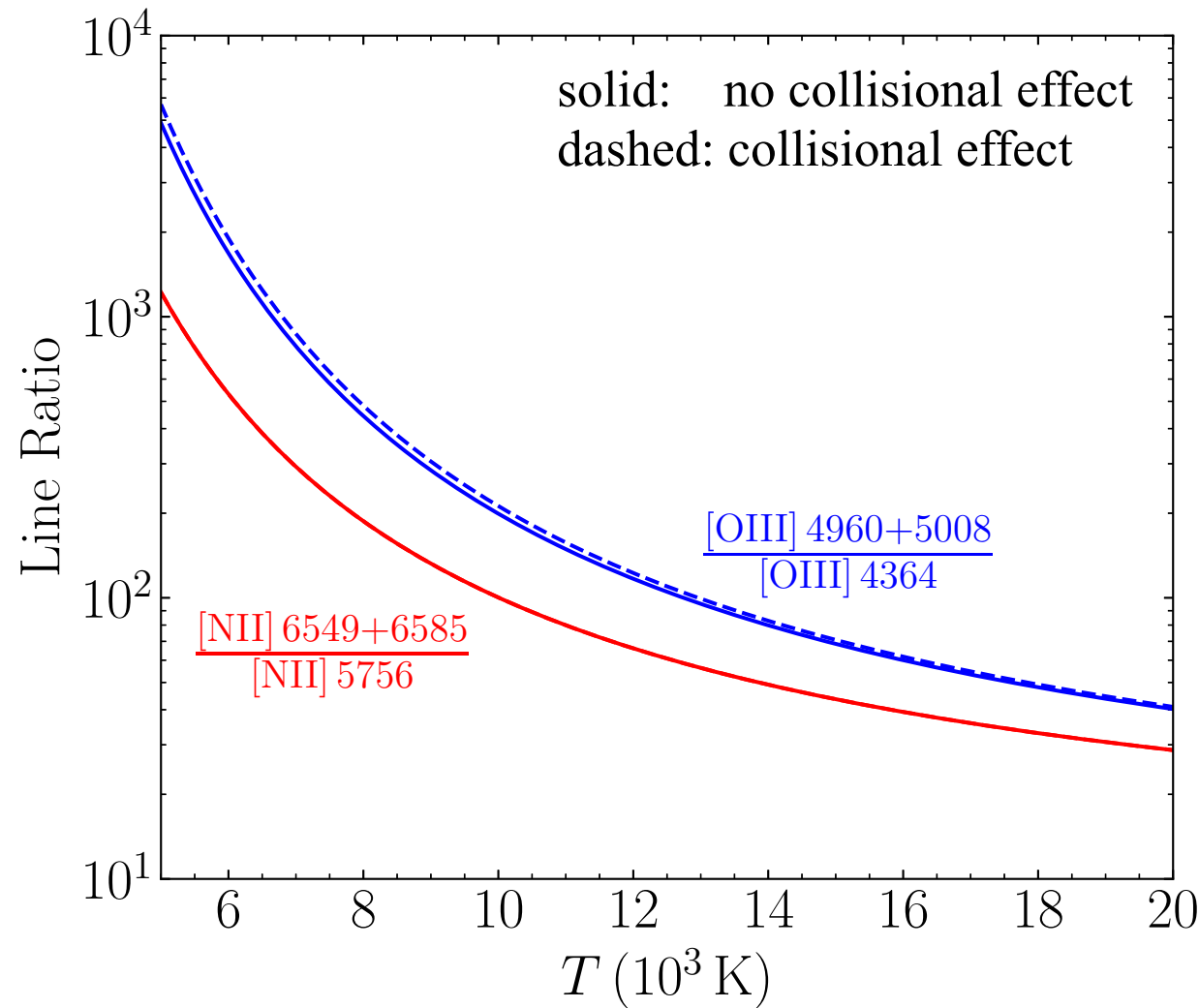
$$\frac{A_{32}}{A_{32} + A_{31} + n_e k_{32} + n_e k_{31}} = \frac{A_{32}}{(A_{32} + A_{31}) \left(1 + \frac{n_e k_{32} + n_e k_{31}}{A_{32} + A_{31}} \right)}$$

$$\frac{A_{43}}{A_{43} + A_{41} + n_e k_{43} + n_e k_{41}} = \frac{A_{43}}{(A_{43} + A_{41}) \left(1 + \frac{n_e k_{43} + n_e k_{41}}{A_{43} + A_{41}} \right)}$$

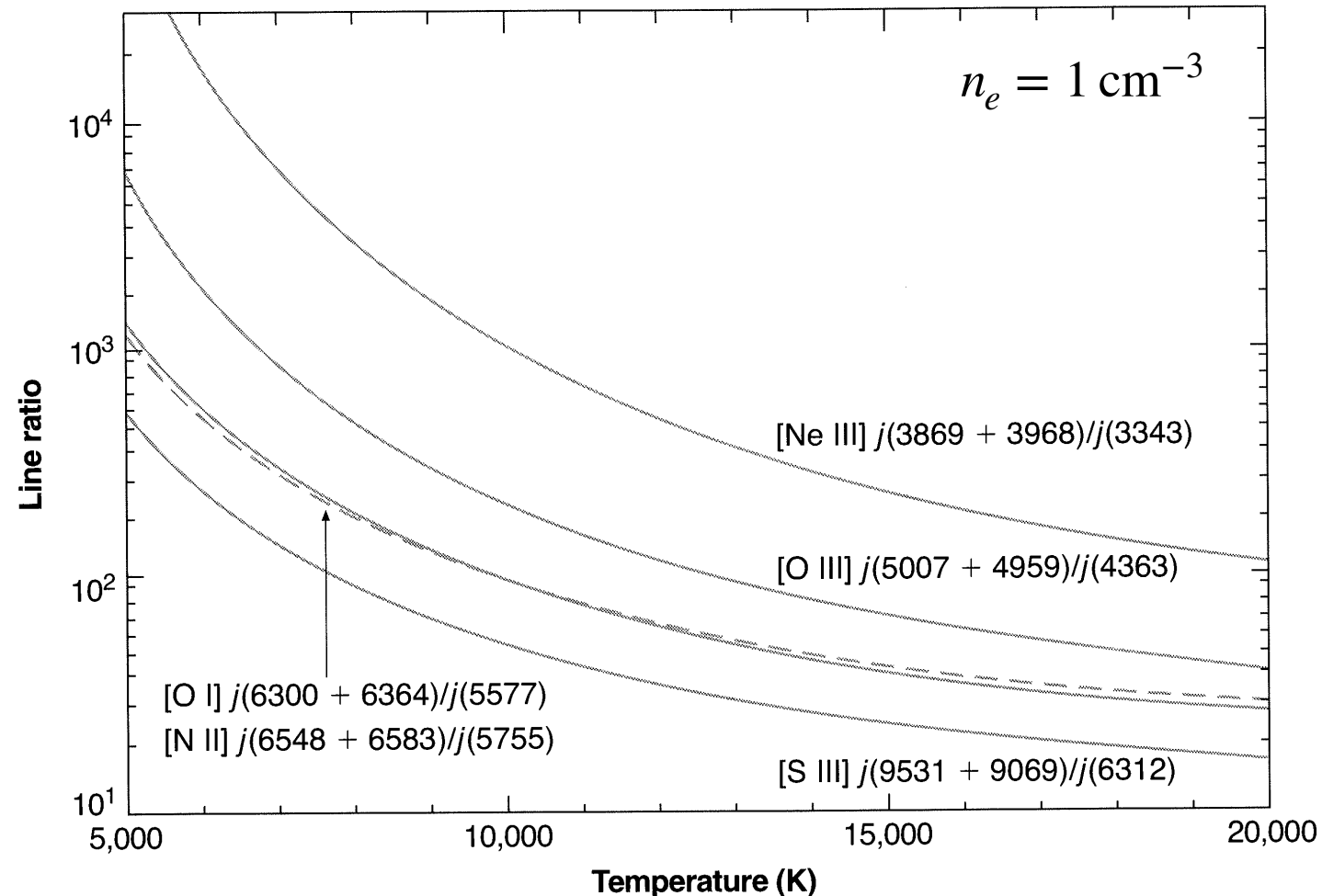
$$\frac{j(3 \rightarrow 1) + j(3 \rightarrow 2)}{j(4 \rightarrow 3)} \simeq \left. \frac{j(3 \rightarrow 1) + j(3 \rightarrow 2)}{j(4 \rightarrow 3)} \right|_0 \frac{1}{f_c} \qquad \qquad k_{ji} = \frac{\beta}{T^{1/2}} \frac{\langle \Omega_{ji} \rangle}{g_j}$$

$$f_c = \frac{1 + \frac{n_e k_{32} + n_e k_{31}}{A_{32} + A_{31}}}{1 + \frac{n_e k_{43} + n_e k_{41}}{A_{43} + A_{41}}} \simeq 1 + n_e \left(\frac{k_{32} + k_{31}}{A_{32} + A_{31}} - \frac{k_{43} + k_{41}}{A_{43} + A_{41}} \right) \qquad \qquad \beta = 8.629 \times 10^{-6}$$

Figure 5.1 [Osterbrock]



See Equations (5.4)-(5.7) for a correction factor for the density effect.



$$[\text{O III}] \frac{j_{\lambda 4959} + j_{\lambda 5007}}{j_{\lambda 4363}} = \frac{7.90 \exp(3.29 \times 10^4/T)}{1 + 4.5 \times 10^{-4} n_e / T^{1/2}}$$

$$[\text{N II}] \frac{j_{\lambda 6548} + j_{\lambda 6583}}{j_{\lambda 5755}} = \frac{8.23 \exp(2.50 \times 10^4/T)}{1 + 4.4 \times 10^{-3} n_e / T^{1/2}}$$

$$[\text{Ne III}] \frac{j_{\lambda 3869} + j_{\lambda 3968}}{j_{\lambda 3343}} = \frac{13.7 \exp(4.30 \times 10^4/T)}{1 + 3.8 \times 10^{-5} n_e / T^{1/2}}$$

$$[\text{S III}] \frac{j_{\lambda 9532} + j_{\lambda 9069}}{j_{\lambda 6312}} = \frac{5.44 \exp(2.28 \times 10^4/T)}{1 + 3.5 \times 10^{-4} n_e / T^{1/2}}$$

-
- Comparison with observations
 - Since the forbidden lines are optically thin, the ratio of emergent intensities are the ratio of the integrals of the emission coefficients along a ray through the nebula.
 - The observed strengths of the lines must be corrected for interstellar extinction, but this correction is usually not too large because the temperature-sensitive lines are relatively close in wavelength.
 - $[\text{O III}] (\lambda 4959 + \lambda 5007) / \lambda 4363$
 - $\lambda 4959 + \lambda 5007$ are strong lines, but $\lambda 4363$ is relatively weak, and is close to Hg I $\lambda 4358$ due to light pollution in the sky.
 - Therefore, the line ratio is quite large and difficult to measure accurately.
 - Early works have been centered on the [O III] lines, because they are in the blue spectral region where detectors are most sensitive, and they are quite bright in typical planetary nebulae.
 - $[\text{N II}]$
 - The lines are stronger in the outer parts of H II regions, where the ionization is lower and the O mostly emits [O II] lines.
 - Most recent works have used all of these lines.
 - $^2D^o$ and $^2P^o$ levels of [O II] and [S II] (see page 4)
 - The two levels can also be used as temperature indicators.
 - They have advantage of lying in spectral regions that are relatively easy to observe, but the lines are widely separated in wavelength so that correction for interstellar dust extinction is larger.

- Temperatures of H II regions
 - The temperatures are in the range 7,000-14,000 K.
 - The abundances of the heavy elements tend to increase inward, resulting in the differences in temperatures.

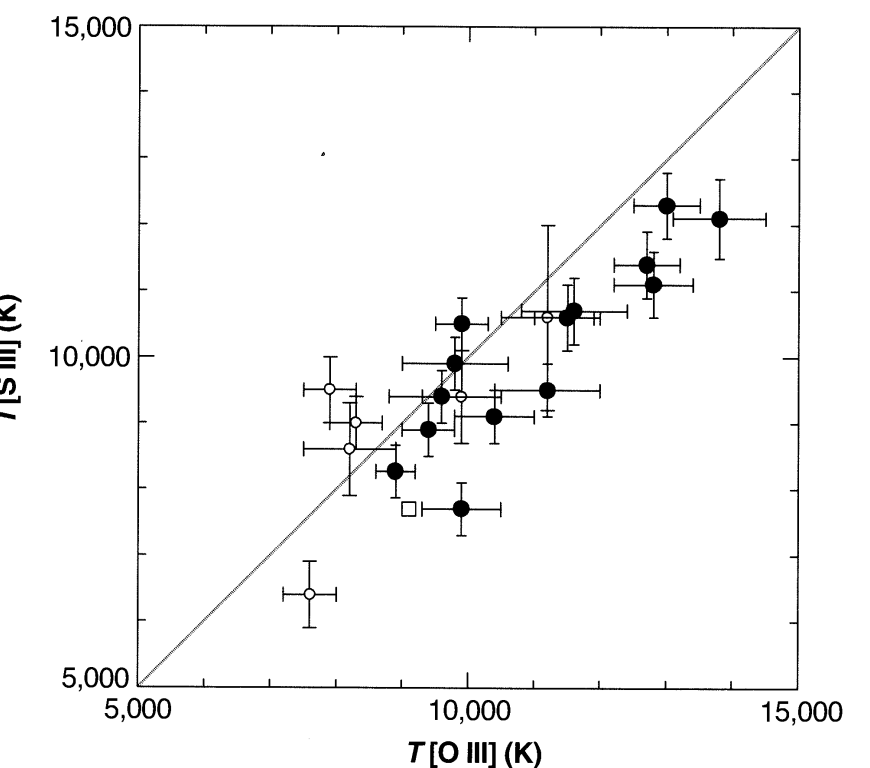
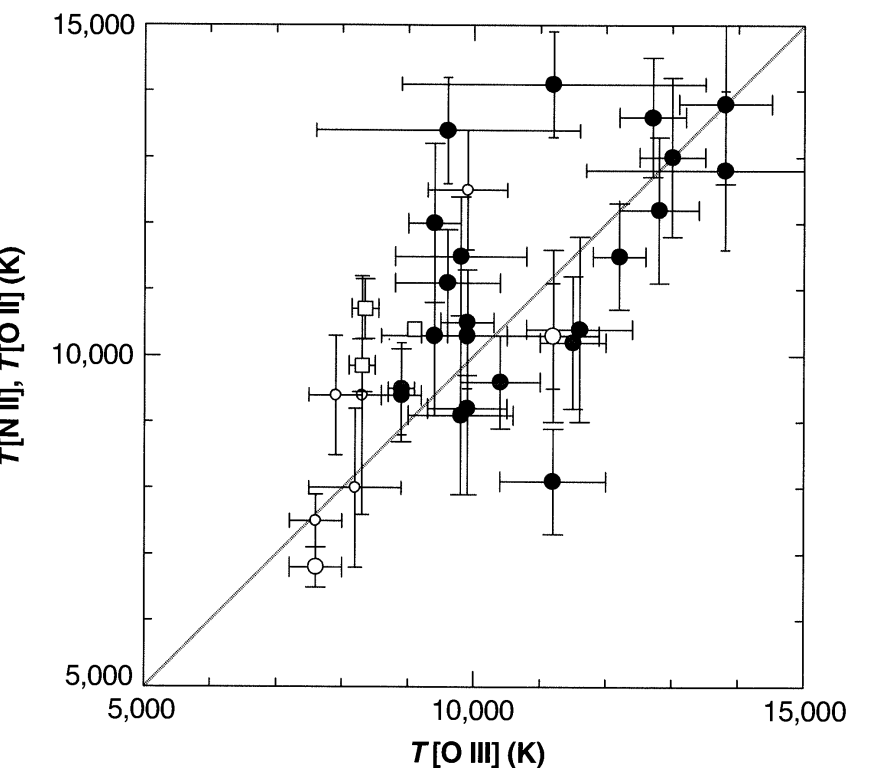


Figure 5.2

A comparison of values of the temperature in H II regions. The closed circles are H II regions in M 101; the open circles, in NGC 2403; and the open squares, different locations in the Orion Nebula.

- Temperature of Planetary nebulae
 - PNe have higher surface brightness than H II regions.
 - Temperatures are measured using [O III].
 - [N II] is relatively weak, but measurements of it are also available.
 - The temperatures in the hottest PNe are somewhat higher than in H II regions, as a consequence of higher effective stellar temperatures and the higher electron densities in PNe, resulting in collisional deexcitation and decreased efficiency of radiative cooling.
 - Halo objects with relatively low heavy-element abundance results in somewhat above-average temperatures due to the lower cooling efficiency.
- It is reasonable to adopt $T \approx 10^4$ K as an order-of-magnitude estimate for any nebula with near-normal abundances.
 - $T \approx 9,000$ K in the brighter parts of an H II region.
 - $T \approx 11,000$ K in a typical bright PN.

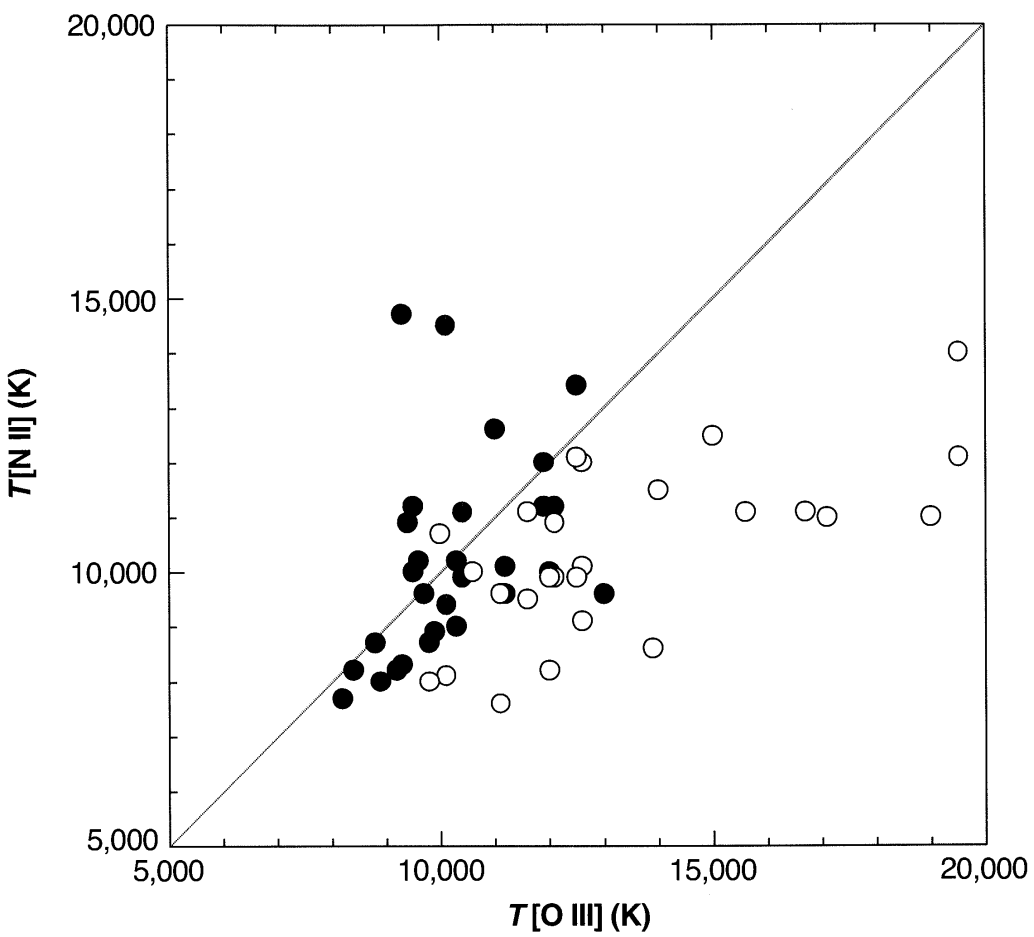


Figure 5.3

A comparison of two temperature indicators for a sample of planetary nebulae.

- Ratio of a collisionally excited line to a recombination line.
 - Another method to determine the temperature is to compare the relative strength of a collisionally excited line, such as C III] $\lambda 1909$, with a recombination line of the next lower state of ionization, such as C II $\lambda 4267$
 - This is because both depend on the product of densities $n(\text{C}^{++})n_e$, which therefore cancels out of their ratios.
 - This method has been applied to relatively few objects because the collisionally excited line usually occurs in the vacuum UV.
 - However, this method has the advantage that the observed ratio is a very powerful function of the temperature so that even modest signal-to-noise spectra can determine the temperature quite accurately

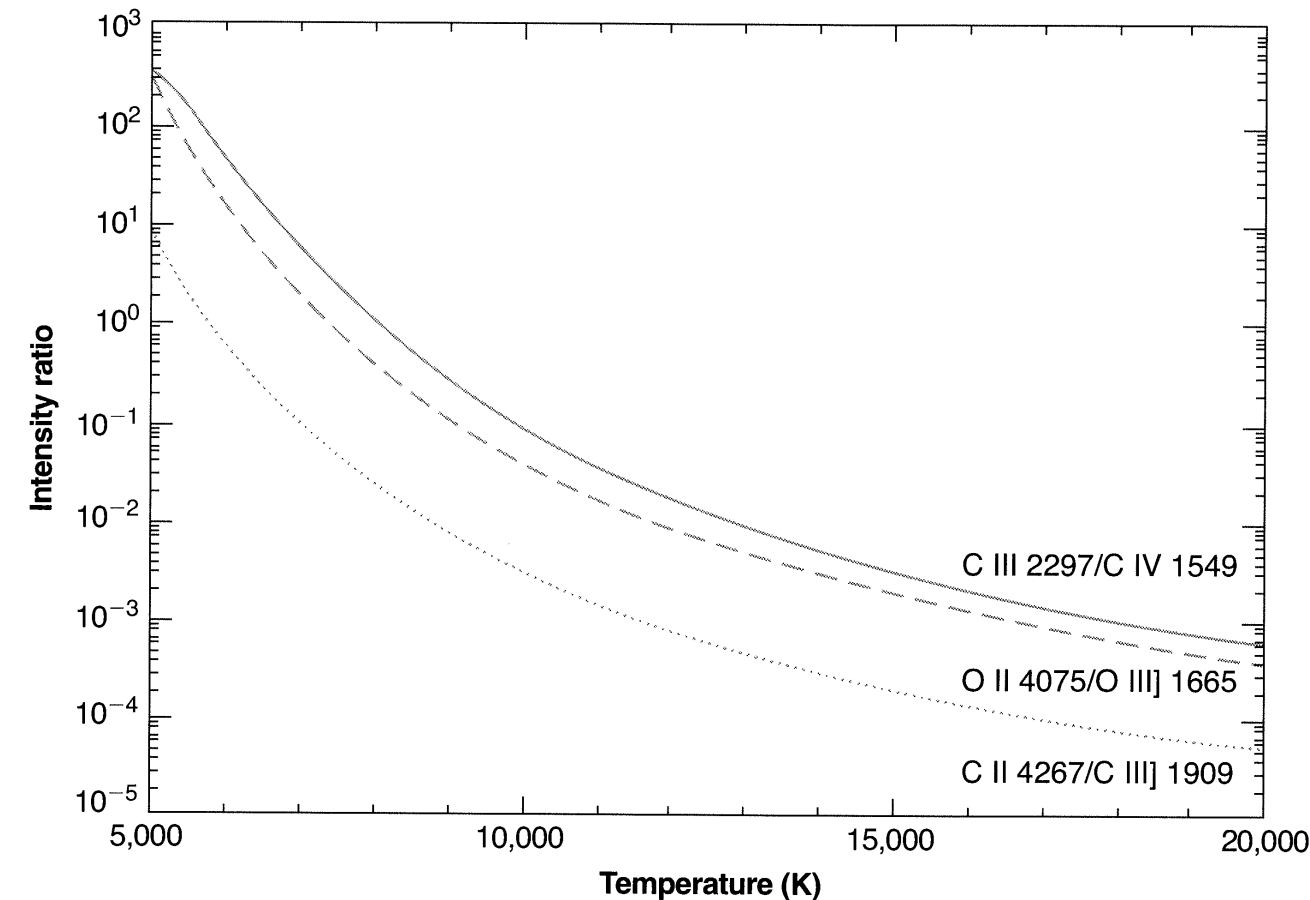


Figure 5.4

Several temperature-sensitive line-intensity ratios of dielectronic recombination to collisionally excited lines.